Theta phase mediates deliberate action switching in human Supplementary Motor Areas

Giovanni Maffei[1,2,*], Riccardo Zucca[1,3], Jordi-Ysard Puigbò[1,2], Diogo Santos-Pata[1], Marco Galli[1], Adrià Tauste Campo[2], Rodrigo Rocamora[2,3], Paul Verschure[1,4,*]

[1] SPECS Lab., Institute of Bioengineering of Catalonia (IBEC), Barcelona Institute of Science and Technology (BIST), Barcelona, Spain

[2] Universitat Pompeu Fabra (UPF), Barcelona, Spain

[3] Epilepsy Monitoring Unit, Department of Neurology, Hospital del Mar Medical Research Institute, Barcelona, Spain

[4] Institucio´ Catalana de Recerca i Estudis Avanc,ats (ICREA), Barcelona, Spain

* Corresponding authors: giovanni.maffei@upf.edu, pverschure@ibecbarcelona.eu

ABSTRACT

The ability to deliberately overwrite ongoing automatic actions is a necessary feature of adaptive behavior. It has been proposed that the supplementary motor areas (SMAs) operate as a controller that orchestrates the switching between automatic and deliberate processes by inhibiting ongoing behaviors and so facilitating the execution of alternative ones. In addition, previous studies support the involvement of SMAs theta waves (4-9 Hz) in cognitive control. However, the exact role of such oscillatory dynamics and their contribution to the control of action are not fully understood. To investigate the mechanisms by which the SMAs support direct control of deliberate behavior, we recorded intracranial electroencephalography (iEEG) activity in humans performing a motor sequence task. Subjects had to perform a "change of plans" motor task requiring habitual movements to be overwritten at unpredictable moments. We found that SMAs were exclusively active during trials that demand action reprogramming in response to the unexpected cue but were silent during automatic action execution. Importantly, SMAs activity was characterized by a distinct temporal pattern, expressed in a stereotypical phase alignment of theta oscillations. More specifically, single trial motor performance was correlated with the trial contribution to the global inter-trial phase coherence, with higher coherence associated with faster trials. In addition, theta phase modulated the amplitude of gamma oscillations, with higher cross-frequency coupling in faster trials. Our results suggest that within frontal cortical networks, theta oscillations could encode a control signal that promotes the execution of deliberate actions.

36 **INTRODUCTION**

37

38 The ability to deliberately interrupt and overwrite ongoing actions as a response to external cues is a

39 necessary feature of cognitive control. For example, when driving a car on a known route, we

40 automatically perform highly trained actions to reach a familiar destination. However, if the habitual

41 route is found blocked, the automatic driving routines are promptly interrupted, and a new motor

42 program is deliberately assembled and selected to follow an alternative path to the goal.

43 The Supplementary Motor Areas (SMAs), in the Medial Frontal Cortex (MFC), are thought to mediate

44 the switch from automatic to deliberate control when a conflict between current and expected

45 contingencies is detected which requires alterations in ongoing actions (1–5). In particular, it has

46 been suggested that the SMAs orchestrate the balancing of automatic and deliberate processes by

47 inhibiting ongoing motor routines to facilitate the execution of alternative deliberate actions (4,5).

48 Animal studies support this hypothesis, for instance, by showing the involvement of neurons in the

49 primate SMAs in either suppressing or promoting action during "change of plans" paradigms (6).

50 Nevertheless, the functional role of SMAs in humans is still under debate. Imaging studies have

51 reported increased activation of the human pre-SMAs and SMAs during action reprogramming but

52 not during automatic action execution (1). This is consistent with rare lesion studies where subjects

53 suffering from focal SMAs damage are able to stop an action but unable to switch between automatic

54 and deliberate control (7). These results suggest that human SMAs are not generally involved in

55 action inhibition but are specifically supporting switching behavior. However, this interpretation

56 seems at odds with findings from human EEG studies showing significant activation of the medial

57 frontal cortex (MFC) during a behavioral conflict. Here, a positive relationship between the power

58 increase in the theta range (4-8 Hz) and response time during high-conflict trials suggests that this

59 frequency band (often termed 'frontal theta') could reflect a generic inhibitory mechanism, possibly

60 acting as a "global brake" on the motor system both pro- and retrospectively (i.e. post-error slowing)

61 (8–10). Hence, the exact role of human SMAs in cognitive control is not clear and pointing to a

62 plurality of possible functions.

63 A second topic of debate pertains to the mechanism through which the SMAs can control action

64 execution. Indeed, although the power of the theta band over the motor system could reflect an

65 inhibitory mechanism, recent evidence suggests that the phasic period of frontal theta is crucially

66 related to performance in cognitive tasks that involve frontal cortical circuits (11). In particular, theta

67 band phase coherence within and across frontal, motor and parietal regions seems to correlate with a

68 higher accuracy in rule-based decision making (12,13) and memory tasks (14), as well as shorter

69 reaction times during attentional paradigms (15). Despite this growing body of evidence, a direct link

70 between theta oscillatory phase and the executive control of action is still missing (although see

71 (16)). In summary, it remains unclear whether the human SMAs are involved in behavioral switching,

72 whether they have an inhibitory or faciliatory role in action reprogramming and what is the neural

2

73　　mechanism is underlying this putative role. To address these questions, we tested the ability to

74　　switch between automatic and deliberate control of action in three (pre-operation) epileptic subjects

75　　with iEEG medial-frontal implants in the supplementary motor areas (BA6). Subjects performed a

76　　variation of the Serial Reaction Time Task (SRTT) (17), a paradigm that requires the execution of a

77　　sequence of repetitive visually-guided key-presses, which becomes progressively automated. In a

78　　small subset of trials, the automatic sequence is unpredictably interrupted by the appearance of a cue

79　　(switch trials), which required the subjects to halt the ongoing action sequence and press an

80　　alternative un-cued key (switch trials).

81　　Consistently with the animal literature (4,6), we find that the SMAs are active during switch trials but

82　　not during automatic ones. We also observe that the response time at the single trial level can be

83　　predicted from the movement related cortical potential (MRCP) (18). Notably, the ability to detect

84　　MRCP peaks at the single trial level allowed us to align the iEEG signals recorded from the SMAs to an

85　　endogenous neural event predictive of behavior. This was crucial to minimize intra- and inter-subject

86　　variability (19) and to unveil the intrinsic neural dynamics independent of an exogenous (i.e. cue

87　　presentation) event-locked analysis (12,20,21). We show that the single-trial theta band phase

88　　coherence (22,23), i.e. the contribution of a single trial to the overall phase consistency across trials,

89　　were predictive of motor performance at the single trial level, with higher phase coherence

90　　correlating with shorter reaction times. Neither amplitude nor power of the MRCP had such

91　　predictive power. To further investigate the neurophysiological link between low-frequency

92　　oscillations and behavior, we computed the cross-frequency coupling between theta phase and the

93　　amplitude of higher frequency activity. This analysis revealed a significant increase of theta-gamma

94　　phase-amplitude coupling associated with shorter response latencies suggesting a modulatory effect

95　　of theta rhythms on local neuronal activity.

96　　Altogether our results directly support the role of human SMAs in the control of action switching.

97　　Moreover, they reveal a possible mechanism of cognitive control based on the entrainment of high-

98　　frequency neuronal events by low-frequency oscillations in a cognitive control version of the nested

99　　frequency theta-gamma code (24). This interpretation provides further support for the growing body

100　　of evidence pointing to the role of phase synchrony and modulation in the theta band as a

101　　fundamental operational mode of frontal executive function.

102

103

104　　**RESULTS**

105

106　　**Task and behavioral results**

107

108　　In order to explore the neural dynamics underlying behavioral performance in deliberate action

109　　switching, three human subjects implanted with intracranial electrodes (iEEG) in the supplementary

3

110   motor areas (SMAs) (fig. 1-B), performed a variation of the serial reaction time task (17,25) (fig. 1-A).

111   The task was composed of two consecutive blocks for a total of 565 trials. The first block (trial 1-60)

112   required the participants to learn to perform a repetitive sequence of key-presses (N=5) on a touch-

113   screen keyboard by tapping on a visual cue (green, presented for 500 msec or until pressed) until

114   they reached automaticity. Automaticity was defined as the decrease of inter-key-interval (IKI) to an

115   asymptotic value, indicating that the subject effectively internalized the motor sequence and did not

116   rely on visual feedback (17) (fig. 1-C). We observed a significant decrease in IKI between early and

117   late training trials (fig. 1-D) (t-test unpaired between trials 1-20 (N=20) and trials 40-60 (N=20):

118   SBJ1, t=5.30, $p<10^{-05}$; SBJ2, t=5.71, $p<10^{-05}$; SBJ3, t=4.08, $p<10^{-03}$) and its variability (fig. 1-E) (t-test

119   unpaired: SBJ1, t=2.21, p=0.04; SBJ2, t=2.45, p=0.02; SBJ3, t=3.28, p=0.004), confirming that the

120   subjects performed the sequence in an automatic manner (26).

121   In the second block of the task (trial 61-565), subjects were required to perform the learned

122   sequence of visually guided key presses. However, these were interrupted by the unpredictable

123   appearance of a switch cue (red circle) at pseudo-random intervals (7 +- 2 sec). When the switch cue

124   appeared, subjects had to interrupt their ongoing automatic motor sequence and press a specific

125   uncued key (fixed for each subject throughout the experiment) as instructed during the training

126   phase (switch trials). Subject 1 and 2 requested to interrupt the experiment prematurely. In total we

127   collected 50 switch trials for SBJ1, 57 for SBJ2 and 80 for SBJ3. Subjects were able to successfully

128   interrupt the ongoing action sequence for most of the switch trials. Switch trials where subjects

129   failed to interrupt the ongoing motor sequence and pressed the next key in the sequence (SBJ1, 14%;

130   SBJ2, 20%; SBJ3, 10%) were excluded from the analysis. The behavioral analysis of the key-presses

131   showed consistently longer response in switch trials compared to automatic response trials (fig. 1-F)

132   (t-test unpaired: SBJ1, t=-39.59, p<0.01; SBJ2, t=-32.96, p<0.01; SBJ3, t=-71.56, p<0.01). This

133   increased latency in response time was accompanied by a greater variability ranging from about 600

134   to 1300 ms (fig. 1-G). Hence, the motor response dynamics in automatic trials were consistent and

135   stereotyped whereas in switch trials subjects were variably faster or slower than their mean

136   performance at each trial. This difference cannot be explained as a learning effect, as we did not find

137   a significant correlation between trial order and switch response latencies (Pearson's correlation

138   coefficient: SBJ1: R=-0.11, p=0.18; SBJ2: R=0.08, p=0.37; SBJ3: R=-0.16, p=0.07). In addition, it cannot

139   be consistently explained by the position of the switch cue within the sequence, which showed a

140   significant effect only in one subject (one way ANOVA: SBJ1: $F_{(2,40)}=2.546$, p=0.091;

141   SBJ2:$F_{(2,43)}=2.002$, p=0.147; SBJ3:$F_{(2,69)}=4.685$, p=0.012). This raises the question whether the

142   difference in performance in automatic and switch trials can be explained in terms of the properties

143   of the neuronal process underlying the control of action switching.

144

145
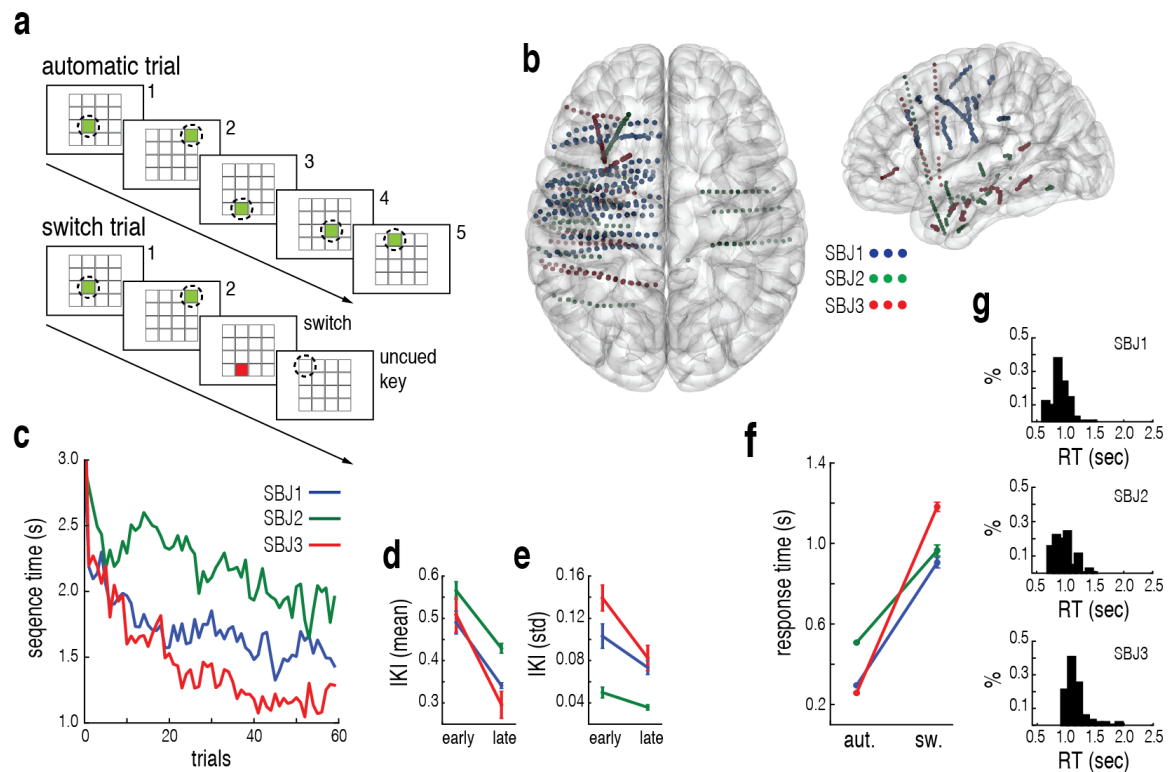
4

Figure 1. Experimental protocol, recording locations and behavioral performance. a. Serial reaction time task. During automatic trials subjects are required to perform a series of visually guided key presses (green key) following a fixed pseudo-randomly generated sequence. During switch trials subjects are presented with a switch cue (red key in a fixed position) appearing at a random step of the sequence, requiring them to interrupt the ongoing motor sequence and press a specific uncued key. **b.** Projection of the locations of relevant contact points in MNI coordinates for each subject. **c.** Evolution of trail duration during training per subject. **d.** Mean Inter-Key-Interval (IKI) in seconds during early (trial 1-20) and late (trial 40-60) phases of training for each subject. **e.** IKI standard deviation during early (trial 1-20) and late (trial 40-60) phases of training for each subject. **f.** Comparison between response time during automatic and switch trials for each subject. Switch responses are collected from all the valid trials in the switch condition from the appearance of the switch cue to the key press. Automatic responses comprise the same number of key presses sampled from the automatic sequence at random from the pool of automatic trials (SBJ 1: N = 43; SBJ 2: N = 46; SBJ 3: N = 72). **g.** Normalized distribution of response time during switch trials for subject. Response time computes as in f.

SMAs are involved in switch but not automatic action

It is believed that the SMAs contribute to cognitive control in particular the switching between automatic and deliberate action (2–4). We validated this hypothesis by training a classifier to identify the trial type (automatic vs. switch), by the signals obtained from all the available contact points for each individual subject (see Methods). This classification shows that the signals obtained from the

5

168 medial-frontal cortex, and in particular the SMAs (BA6C), are most predictive of switch trials (F1
169 score=0.7) followed by the motor cortex (BA4) (F1 score = 0.57) and the lateral premotor cortex
170 (B6L) (F1 score = 0.52). In particular, we observe that the amplitude of the iEEG local field potentials
171 (LFPs) measured in the SMAs is predictive of the type of trial (automatic or switch) (fig. 2-A, B).
172 Following this step, we restricted our analysis to the relevant contact points in the SMAs in order to
173 determine the precise role of SMAs in switching from automatic to deliberate behaviors.
174 Analyzing the time evolution of the SMAs iEEG we observe that during switch trials, a significant
175 movement related cortical potential (MRCP) preceded the response in all three subjects. In contrast,
176 this MRCP was not present during automatic trials (T-statistics cluster permutation (N=1000)
177 analysis: SBJ1, t=34.09, $p<10^{-4}$; SBJ2, t=21.20, $p<10^{-4}$; SBJ3, t=29.69, $p<10^{-4}$) (fig. 2-B). To control
178 whether this MRCP encoded the motor sequence initiation rather than a switch action per se (27), we
179 aligned the LFPs for each subject to the cue indicating the beginning of the automatic motor sequence
180 (not shown). We found no significant increase in amplitude confirming that the earlier observed
181 MRCP was specific to automatic-deliberate switching (T-statistics cluster permutation (N=1000)
182 analysis: SBJ1, t=7.64, p=n.s.; SBJ2, t=4.73, p=n.s.; SBJ3, t=8.13, p=n.s.).
183 Our results confirm that the SMAs mediate the execution of actions that require cognitive control,
184 such as switch trials and are not involved in the control of over-trained sequential motor responses
185 nor the initiation of automatic sequences (1).
186 Due to the high resolution of intracranial EEG, we aimed to identify robust MRCPs at the single trial
187 level in order to determine what features of the neural signal were predictive of behavioral
188 performance. To achieve this, we extracted the temporal and amplitude information for each event
189 by band-pass filtering the signal at low frequencies (1-2 Hz) and further extracting the absolute peak
190 (fig. 2-C-1,2) (18,28). We further analyzed the time window from the switch cue presentation to the
191 MRCP peak (TP), the time window from the peak to the key press (FP) and the peak amplitude (A) in
192 relation to the response time at each trial. Temporal analysis of the MRCP showed a marked
193 correlation between its time to peak (TP) and reaction time with respect to cue presentation at the
194 single trial level (Pearson's correlation coefficient: SBJ1, R=0.481, p<0.001; SBJ2, R=0.779, $p<10^{-10}$,
195 SBJ3, R=0.499, $p<10^{-5}$) (fig. 2-E). A similar positive correlation was found between single trial time-
196 from-peak to key-press (FP) and the response time (Pearson's correlation coefficient: SBJ1, R=0.698,
197 $p<10^{-7}$; SBJ2, R=0.707, $p<10^{-8}$, SBJ3, R=0.464, $p<10^{-5}$) (fig. 2-F). In contrast, peak amplitude showed
198 no consistent effect on response times and only in one subject reached statistical significance
199 (Pearson's correlation coefficient: SBJ1, R=0.141, p=0.371; SBJ2, R=0.314, p=0.035, SBJ3, R=0.06,
200 p=0.959) (fig. 2-G). To further quantify the relevance of the time to peak and amplitude aspects of the
201 MRPC for switch behavior we fit a linear model for each variable and computed the explained
202 variance (R^2) with respect to
203
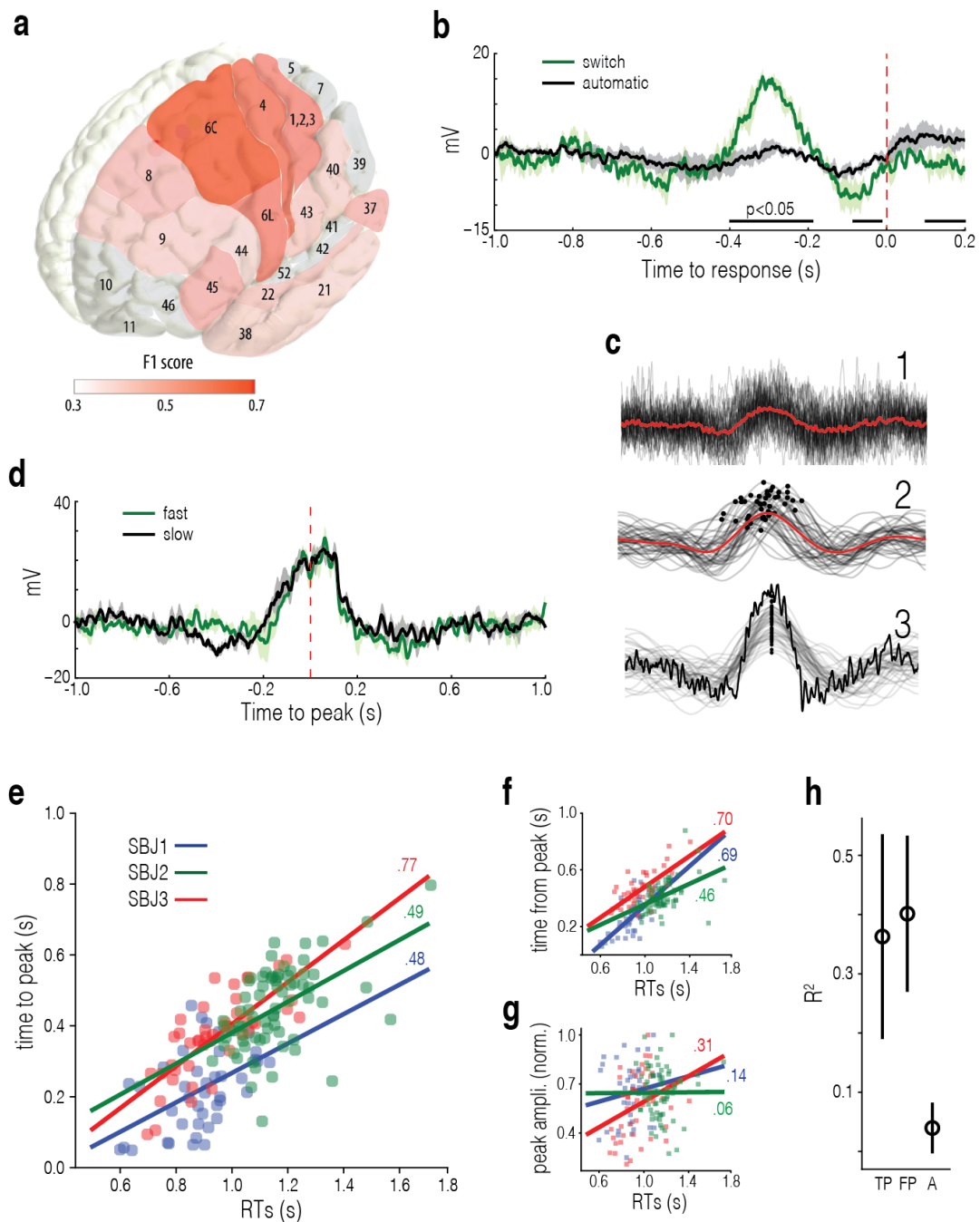
Figure 2. Neural response in SMAs. **a.** Classifier mean prediction accuracy of switch trials projected over a Brodmann atlas. Red hue represents the classification accuracy (F1 score) associated with the areas that were recorded, gray denotes areas not present in the recording. **b.** Motor Related Cortical Potential (MRCP) in SMAs during switch (green) and automatic (black) trials aligned to motor response (red dashed). Switch trials are aligned to the key-press in response to the switch cue (key press of the uncued key), automatic trials are aligned to the last key-press of the automatic sequence. Mean and SEM for each subject. Bar indicates the intersection of

212 significant temporal windows for all the subjects (p<0.05). **c.** Example of alignment of single trial MRCPs to the

213 relative peak for one subject. 1. Key-press aligned MRCPs for each switch trial (black) and mean (red). 2. 2Hz

214 Low passed MRCPs for each trial (black) and mean (red). Black dots indicate the detected peaks. 3. Alignment of

215 low passed filtered MRCPs by their relative peak and unfiltered average. **d.** MRCP in SMAs during fast and slow

216 responses during switch trials (trials sorted by the median of the response time distribution) aligned to the peak

217 of the band-passed MRCP (red dashed). Mean and SEM of subjects**. e.** Relationship between time of response and

218 of cue presentation to MRCP peak during switch trials for each subject. Solid line indicates the linear fit of the

219 data and Pearson's correlation coefficient. **f.** Relationship between response time and time from MRCP peak to

220 key-press during switch trials for each subject**. g.** Relationship between response time and MRCP peak

221 amplitude during switch trials for each subject. **h.** Mean R^2 linear regression coefficient between response time

222 and time from cue to peak (TP), time from peak to key-press (FP) and peak amplitude (A). Each score is obtained

223 on the test set as a result of an independent regression for each regressor trained on 70% of the available

224 aggregated trials and tested on the remaining 30%. Mean scores and standard deviation are the result of a 100-

225 fold cross-validation.

226

227 the response time (fig. 2-H). This analysis confirmed that the temporal dynamics of the MRPC in

228 terms of time-to-peak from cue onset and time-from-peak to response could accurately predict

229 performance while excluding amplitude as a reliable predictor of motor behavior.

230 We subsequently analyzed whether the profile of the MRPCs showed any behavior dependent

231 modulation by comparing fast and slow switch trials (fig. 2-D). For each subject, trials were aligned to

232 the time of the peak of the band-passed MRCP (as shown in fig. 2-C-3). Further, these trials were

233 sorted into two groups according to the median value of the response time distribution (i.e. fast and

234 slow) in order to obtain an equal number of trials for each group and potential differences between

235 groups tested using cluster-based permutation analysis. This analysis revealed no differences

236 between fast and slow switch trials (T-statistics cluster permutation (N=1000) analysis: SBJ1, t=5.87,

237 p>0.05; SBJ2, t=9.23, p>0.05; SBJ3, t=8.61, p>0.05) suggesting that, although the MRPC is a

238 characteristic neural signature of switch actions, it does not encode information predictive of

239 behavioral parameters such as response time.

240 Altogether, these results suggest that the SMAs are recruited for deliberate control of switching

241 behavior and that the temporal features of the MRPC, i.e. phase, are decisive in controlling the

242 response time (29).

243

244

245 **Theta phase aligns in faster actions**

246

247 We hypothesized that oscillatory dynamics in the theta range could constitute a neural signature of

248 cognitive control by mediating deliberate action switching. Previous reports have suggested a strong

249

8

250
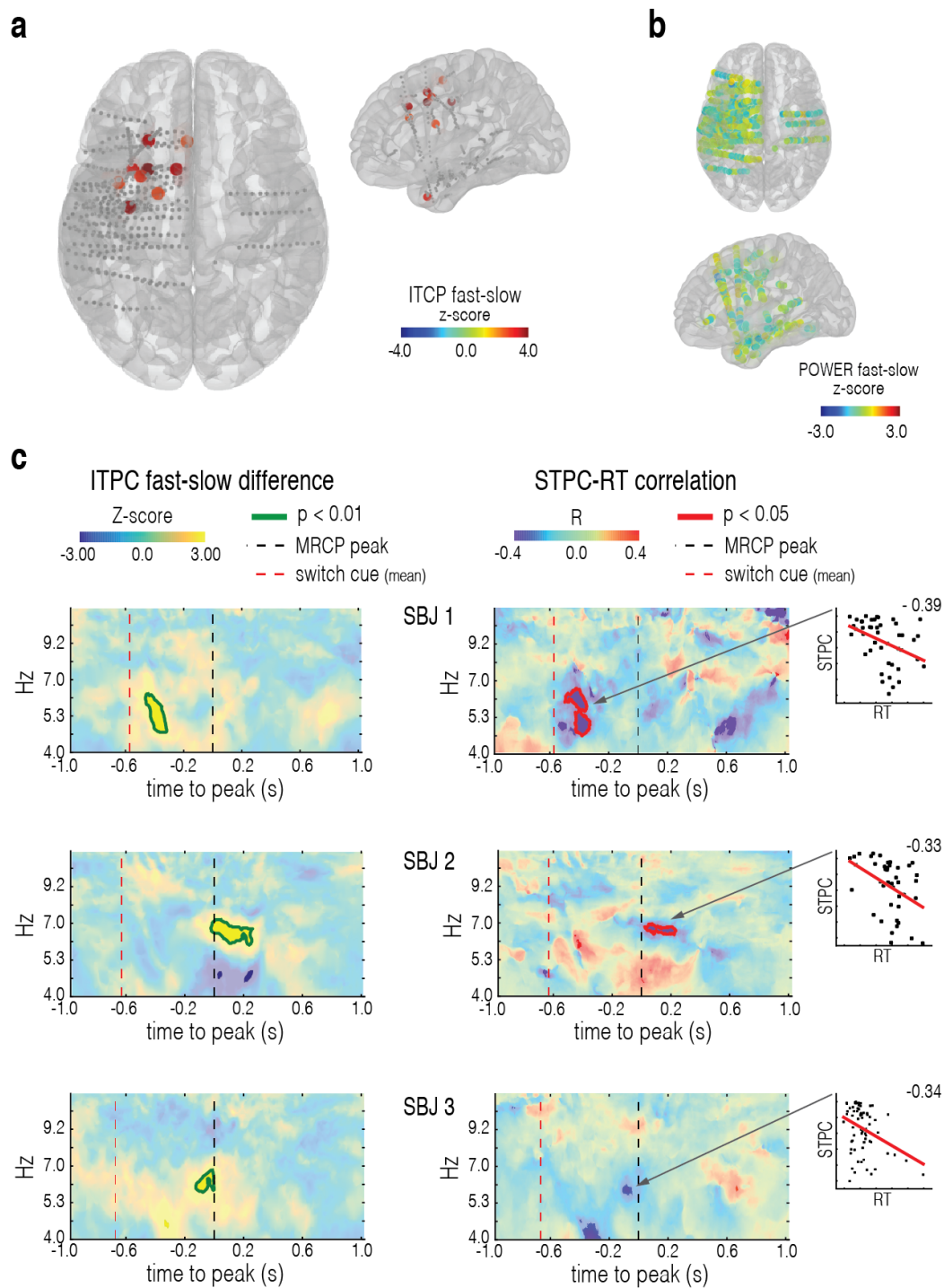
Figure 3. Phase alignment and performance. a. Inter-trial phase coherence difference (z-score) between fast and slow (fast-slow) switch trials for the combination of the significant contact points for each subject projected on the MNI space. Contact points showing a significant cluster of time-frequency bins (z > 2.58, Montecarlo p value < 0.05) in the time window –1 s to 1 s centered to the peak of the MRCP are represented in color. **b.** Power

9

257   difference (z-score) between fast and slow (fast-slow) switch trials for the combination of all the contact points

258   available from all the subjects projected on the MNI space. No contact point reached a statistically significant

259   level, therefore no masking is applied to this figure. **c.** Single subject statistical analysis. **left.** ITPC normalized

260   difference between fast and slow (fast-slow) switch trials. Trials are aligned by the relative peak of the MRCP

261   (black dashed line). Red dashed line indicates the average cue onset time with respect to MRCP peak. Green

262   outline indicates region with Monte Carlo P value < 0.01. **right.** Spearman's R correlation coefficient between

263   Single Trial Phase Coherence (STPC) and Response Time (RT) computed for each time frequency bin during

264   switch trials. Trials are aligned by the relative peak of the MRCP (black dashed line). Red dashed line indicates

265   the average cue onset time with respect to the MRCP peak. Red profile indicates Monte Carlo P value < 0.05. **box.**

266   Relationship between Response Time and STPC for the significant area shown in the time-frequency plot shown

267   to the left. Red line indicates linear fit.

268

269   implication of phase dynamics in cognitive control (11,12,16) suggesting the possibility that

270   stereotypical phase profiles could underlie deliberate action modulation.

271   To detect potential stereotypical phase patterns underlying the differences in response times (RT),

272   we first aligned the LFPs to the peak of the MRCP. Note that this is not only a necessary step to filter

273   out inter- and intra- subject differences so as to compare phase profiles across conditions (19), but it

274   could also reveal oscillatory patterns that are removed when using exogenous events as reference

275   (8,12,20). Further, we sorted the switch trials for each subject into two classes of equal size (*fast* and

276   *slow*), by splitting the RT distributions by their median value. For each subject and each available

277   contact point, we then calculated ITPC for fast and slow trials and computed the normalized phase

278   coherence difference following the method described in (30) (see Methods).

279   Class comparison revealed a significantly larger phase alignment in fast trials compared to slow trials

280   localized in the SMAs for all the subjects. To verify the specificity of this result we applied Z-statistics

281   cluster permutation analysis to all the available contact points in order to identify significant

282   differences in ITPC between fast and slow trials (see Methods) and further projected in MNI space

283   the contact points with a significant difference (p < 0.05) in the time window between -0.6 and 0.4 s

284   with respect to the peak of the MRCP (Figure 3-A, see Methods). We observe that, contact points with

285   significantly stronger phase alignment fall in between Brodmann area 6 and 9 for subjects 1 and in

286   Brodmann area 6 for subjects 2 and 3. This effect was found in the theta frequency range between 4

287   and 8 Hz (fig. 3-C left for an example for each subject) with an onset varying across subjects between

288   0.5 and 0.1 seconds before the MRCP peak, possibly due to implant location differences (i.e. more

289   frontal for subject 1). Similar theta range variability was detected in the contact points of individual

290   subjects in areas anatomically or functionally related to the SMA. In particular, in the anterior

291   cingulate cortex (ACC) of subject 3 and in the temporal lobe of subject 2 (see Table 1 for a list of the

292   contact points with significant differences (p < 0.05) in phase alignment between fast and slow

293   trials).

10

294   To further confirm the role of theta phase dynamics with respect to action switching, we applied a
295   single-trial analysis to a subset of contact points in the SMAs that showed the reaction speed and
296   phase alignment effect. Our specific goal was to determine the contribution of inter-trial phase
297   coherence to motor performance. In particular, we computed the total inter-trial phase coherence
298   (ITPC) for each time-frequency bin and inferred the individual contribution of intra-trial coherence
299   by computing a Single Trial Phase Coherence (STPC) pseudo value following (22,23). Finally, for each
300   time-frequency bin, we computed a Spearman's R correlation between the trial response times (RT)
301   and the relative STPCs (see Methods). We observe a negative correlation between RT and STPC in the
302   4-8 Hz frequency band once aligned to the peak of the MRCP (fig. 3C, right) (Z-statistics cluster
303   permutation (N=1000) analysis: SBJ1, z>1.96, p<0.001; SBJ2, z>1.96, p<0.001; SBJ3, z>1.96, p=0.07).
304   Altogether these analyses reveal a stereotypic phase profile of theta oscillations locked to the motor
305   potential controlling action switching whose magnitude is monotonically related to the time of the
306   behavioral response at the single trial level.
307   Importantly, it has been argued that phase coherence may be induced by increases in the power of
308   the oscillations, thus constituting an evoked rather than an actual phase alignment (29). We
309   controlled for this possibility by calculating the difference in power between fast and slow trials and
310   compared the obtained z-scored differences with those obtained in the ITCP domain (fig. 3-B). This
311   analysis confirms a significant effect of ITPC on response time in the absence of significant
312   differences in power suggesting that the detected phase alignment is likely the result of an actual
313   phase coding mechanism within the theta range.
314   Altogether, these results suggest that the SMAs play a central role in controlling the ability to switch
315   from the execution of an automatic motor sequence to the execution of a deliberate action prompted
316   by an unexpected cue. The enhanced synchronization of theta frequencies in faster switch trials, in
317   absence of power differences, supports the role of phase dynamics as a mediating mechanism that
318   facilitates the execution of deliberate movements. In addition, the differences found in the ACC and
319   temporal lobe support the existence of a functional network involved in switching. Within this
320   network the ACC could be responsible for selectively biasing processes in favor of task relevant
321   information during high conflict switch trials (31). The temporal lobe in turn might encode for
322   arousal or surprise elicited by the unexpected cue (32,33)or support the mnemonic aspects of the
323   decision making process (e.g. retrieving what key should be pressed once the cue is presented) (34).
324

Subject	Contact point	MNI coordinates	Brodmann Area	ITPC statistics
1	I'12	-23,713;25,731;35,165	BA9	Z=3.547, MC_p=0.004
2	T'3	-32,098; 10,264; -38,737	BA36	Z=3.210, MC_p=0.022
2	X'10	-24,089; 10,467; 38,760	BA6	Z=4.003, MC_p=0.014

11

3	K'2	-8,865; 10,540; 47,061	BA32	Z=3.546, MC_p=0.016
3	O'10	-39,712; 3.550; 30,963	BA48	Z=2.841, MC_p=0.026
3	M'9	-33,840; -9,556; 39,289	BA6	Z=3.737, MC_p=0.022
3	R'4	-18,703; -2,314; 56,739	BA6	Z=2.836, MC_p=0.04
3	K'7	-27,784; 6,911; 42,980	BA6	Z=3.005, MC_p=0.046
3	B'1	-3,148; 25,277; 26,200	BA32	Z=2.727, MC_p=0.042

Table 1. List of all the contact points where the difference in ITCP between fast and slow trials reached statistical significance.

Cross-frequency coupling predicts faster movements

We have shown that the speed of deliberate action switching is accompanied by theta phase alignment. However, the direct physiological link needed to support the hypothesis that theta phase dynamics modulate performance via phase-dependent neural activity needs to be established. We sought to answer this question by determining the modulatory effect of theta phase on local high-frequency activity with the hypothesis that higher modulation could support faster switch actions (fig. 4-A), an analysis for which a measure of cross-frequency Phase-Amplitude Coupling (PAC) is particularly suited (35,36).

We restricted our analysis to the contact points and the temporal windows of approximately 400 ms where a significant increase in phase alignment was detected (Figure 3C). To achieve the temporal resolution necessary for this type of analysis we obtained one surrogate signal for fast and slow trials for each subject by concatenating the respective single trial windows for all the SMAs contact points for each subject (see Table 1 for a list of contact points). Further, we computed PAC values (using the GLM approach (37)) between 4-8 Hz phase (modulatory frequency) and the amplitude of higher frequencies (10-100 Hz in steps of 2 Hz, modulated frequency), and obtained the difference between the two types of trials. Further, to test the significance of the difference between fast and slow trials, we computed the expected difference in PAC under the null hypothesis by shuffling the two types of trials and extracted the z threshold corresponding to p=0.01 (38) (see Methods). We observed an increased modulatory effect of the theta oscillatory phase on the amplitude of frequency bands in the low gamma range (30-80 Hz), which was consistent across subjects (Z-statistics permutation (N=1000) analysis: SBJ1, z>2.58, p=0.027; SBJ2, z>2.58, p=0.034; SBJ3, z>2.58, p=0.029, fig. 4-B,D). In addition, a significant modulatory effect was found in the beta range (i.e. 30 Hz) for one subject (SBJ1, z>2.58, p=0.019). Further analysis revealed no difference in absolute gamma amplitude between trial

12

354   types (SBJ1, p=0.23; SBJ2, p=0.26; SBJ3, p=0.65), suggesting that the magnitude of phase modulation,

355   rather than activity *per-se*, has a direct effect on controlling performance (fig. 4-D). This result

356   supports a neurophysiological link between theta phase coherence and deliberate control of the

357   action switching through the modulation of high-frequency activity, often interpreted as a correlate

358   of local population activity (35).
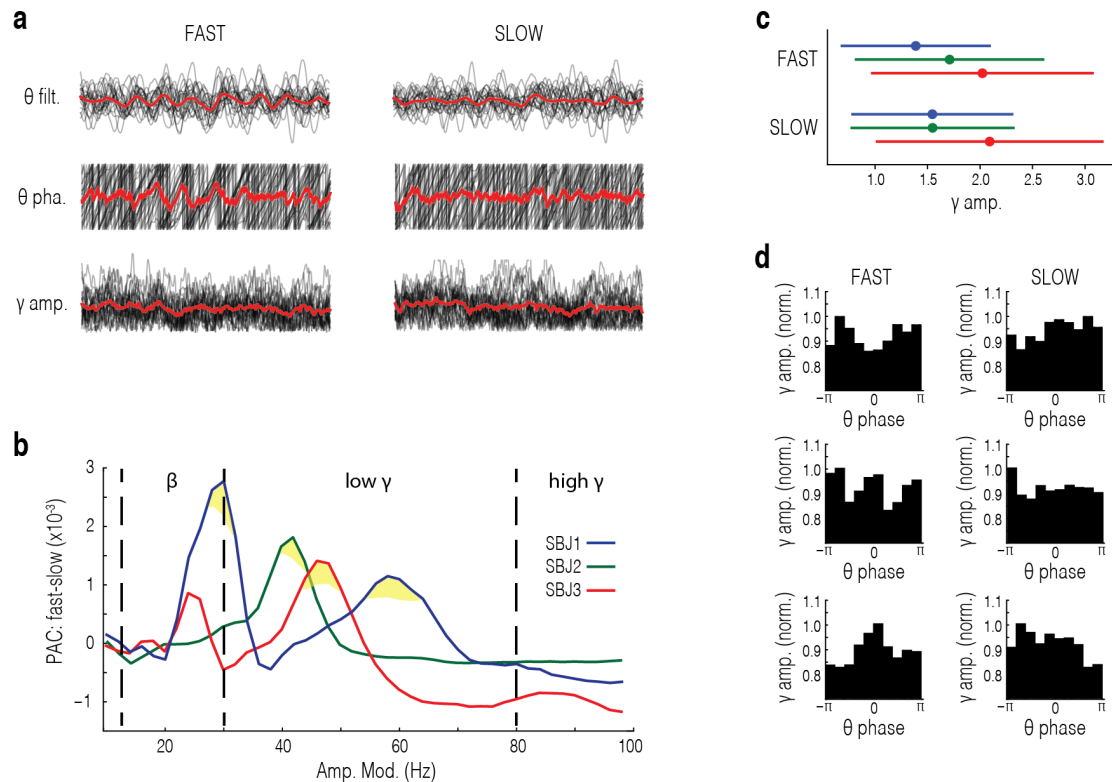
359
360
361   **Figure 4. Theta-gamma cross frequency coupling and its relation to performance.** **a.** Example of
362   oscillatory activity in SMAs during fast trials (left) and slow trials (right) for SBJ 2. Top. LFP traces of individual
363   switch trials (black) and mean (red) filtered in the theta range (4-8 Hz). Center. Oscillatory phase of the
364   individual LFP traces (black) and mean (red) shown in the above panel. Bottom. Amplitude of the individual LFP
365   traces (black) and mean (red) filtered in the low gamma range (30-80 Hz). All traces are aligned to the peak of
366   the MRCP and sorted by fast (< 900 msec) and slow (> 900 msec) response time. **b.** Difference in phase
367   amplitude coupling (PAC) between fast and slow trials (fast-slow) for each subject comparing the phase of theta
368   oscillations (4-8 Hz) to the amplitude of higher frequency bands (x, 30 Hz, 30-80Hz, and 80-100 Hz). Yellow area
369   indicates $p < 0.05$. **c.** Quantification of mean gamma amplitude in fast and slow trials for each subject selected
370   from statistically significant regions marked in yellow in panel b. Bar indicates standard error of the mean. **d.**
371   Distribution of gamma band amplitude (selected from statistically significant regions in b) over the phase of
372   theta for fast (left) and slow (right) trials for each subject.

373
374
375   **DISCUSSION**

376

377 Switching from automatic to deliberate behavior in response to environmental cues is a key aspect of
378 adaptive behavior, however, the substrate and dynamics supporting this ability in the human brain
379 are not fully understood. Here, we have addressed this question by analyzing the iEEG of the
380 neocortex subjects engaged in a switch task. We designed a variation of the Serial Reaction Time
381 Task (SRTT) where automaticity is detected as a progressive shift towards faster and more
382 stereotyped movements, indicating that sequences are performed on the basis of an internal habitual
383 representation and allowed to execute autonomously (7,39,40). Using a classifier of the time-domain
384 features of the iEEG we localized a predictive signal of switch trials to the SMAs which confirmed its
385 role in action control. We found that by aligning trials to action initiation, stereotypical phase profiles
386 in the theta range emerged in the SMAs that predicted switch performance at the single trial level. In
387 addition, we showed that theta rhythms modulated high-frequency power in a performance-
388 dependent manner.

389 In our design, however, we extended the SRTT by introducing a switch cue the required the subjects
390 to interrupt the automated sequence and execute an alternative key-press. This alternative action
391 was un-cued, and it occurred at a low and variable rate, at unexpected positions in the sequence, in
392 order to both avoid habituation and maintain active deliberation. This manipulation is analogous to
393 the switch cue used in (6). However, in our setup, the alternative action was un-cued, to guarantee a
394 minimum amount of deliberation since subjects had to retrieve and implement a specific instruction
395 set from memory (5). During the switch trials, we found significantly longer response times,
396 suggesting a switch from automatic to controlled, deliberate processes (3,6,41). Within the
397 psychological literature, this behavioral marker is known as switch cost (42), interpreted as the
398 result of an "act of control" that involves attentional, mnemonic and motor processes.

399 We found that activity in the SMAs could successfully predict whether the action was performed
400 deliberately or automatically, supporting the involvement of human SMAs in executive control. This
401 result extends previous evidence from primate studies that demonstrated a lateralized increase in
402 the firing rate of supplementary eye field neurons that exclusively accounted for successful
403 performance during switch but not automatic actions (4). Although the activity profile found in our
404 study is qualitatively similar to the one reported in (6), it remains unclear what the
405 neurophysiological link between low-frequency LFP events and firing rate is. One possibility is that
406 the motor potential we reported (fig. 2-b) is the result of the sum of synchronized
407 afterhyperpolarization events of SMAs neurons contributing to the extracellular field potential (43).
408 This pattern of activity is also consistent with human fMRI studies that reported a consistent
409 activation of the SMAs and the more anterior pre-SMAs during action switching (1,41,44). For
410 example, SMAs are transiently active, together with the cingulate cortex, during the execution of
411 switch actions triggered by response conflict (1,45). Besides, TMS induced inhibition of medial
412 frontal areas impaired the ability to switch between motor responses but not the ability to initiate

14

413   action per se, an observation consistent with our results showing no significant change of activity
414   during sequence initiation (46). Moreover, contrary to previous reports (27), we excluded the
415   possibility that the neural signature of switching we report could encode sequence production, as no
416   SMAs activity was found during automatic trials. Instead, we demonstrate, to the best of our
417   knowledge, for the first time the movement-cortical potential (MRCP) as the prominent signature of
418   deliberate action switching in the human SMAs using iEEG. MRCPs are low-frequency potentials
419   generated in association with the planning and execution of a cued or self-paced voluntary
420   movement in premotor and motor regions (18). MRCPs can be decomposed in three distinct
421   components: a slow rise component, known as Readiness Potential, which is more prominent in self-
422   paced movements (47,48). A fast decay component following the RP, called negative slope (NS),
423   which peaks at the moment of maximum negativity in concomitance of action initiation (motor
424   potential - MP). Finally, a rebound activity following movement initiation is associated with
425   movement monitoring. In our task, we identified a strong NS component preceding movement
426   initiation but no clear RP, possibly because the switch action was not internally (i.e. voluntarily)
427   generated. Previous literature indeed shows more prominent NS and absence of RP in cue-guided
428   movements compared to self-paced ones (49).

429   The absence of RP could also support a recent hypothesis by Schurger and colleagues (50). They
430   suggest that this apparent signature of volitional control could be attributed to an artefact arising
431   from the averaging of stochastic fluctuations in the neural activity over trials. Indeed, within the EEG
432   literature MRCPs are typically extracted from averaging across a large number of trials time-locked
433   to action initiation, in order to filter out the noise and account for artefacts introduced by scalp
434   diffusion (51). This procedure, however, generates an artificial build-up in the averaged signal that
435   reflects the integration of noise in a stochastic decision process (SDP) following a drift-diffusion
436   model, where neural activity reaches a "decision threshold" and drives action initiation due to the
437   combination of evidence and stochastic fluctuations. The latter is seen as the source of the variability
438   in response times (52). In our study, the higher resolution and low SNR of iEEG allowed to robustly
439   detect MRCPs at the single trial level directly from the neural tissue and to extract reliable MRCPs
440   features. This allowed for a single-trial analysis precluded in standard EEG analyses usually deployed
441   in the investigation of RP (8,20,21) that support the SDP hypothesis. From a time-domain
442   perspective, the key finding in the single trial analysis of switch trials is that the temporal aspects of
443   the MRCP peak, but not its amplitude, could accurately predict switch response times. This is at odds
444   with previous EEG reports that showed a significant difference in the amplitude of cortical potentials
445   depending on the speed and strength of the movement (53,54). The difference between our and
446   previous results could be due to the different methods employed in the recording. LFPs indeed
447   represent the extracellular activity of neural populations, and they closely track responses in a
448   restricted area of the neural tissue. EEG, in turn, captures a more spatiotemporally extended yet

15

449   attenuated LFP that integrates several square millimeters of superficial cortical activity and it may

450   reflect more diffuse macroscopic effects (43).

451   Another methodological advantage of detecting single-trial time domain features is the possibility to

452   align individual trials to the dynamics of endogenous events. This is a necessary step to compare

453   oscillatory patterns across different conditions and subjects, as it has been shown that phase

454   synchrony measures are sensitive to inter-subject and intra-subject temporal variability (19). In

455   addition, previous studies have shown that locking to endogenous events rather than to exogenous

456   ones (i.e. stimulus presentation) can reveal important and otherwise hidden dynamics (12). By

457   aligning individual trials to the MRCP peak, we found that phase synchrony in the theta band across

458   trials predicted switching actions, where higher synchrony is associated with faster trials. This result

459   suggests that action initiation is locked to stereotypical phase profiles in the theta range, suggesting a

460   mechanism by which neurons in the medial frontal cortex synchronize to convey cognitive control

461   signals to downstream motor areas. This also defines a contrast between our results and the SDP

462   hypothesis, by virtue of analyzing signals relative to an internal reference, i.e. MRCP, we reveal a

463   systematic phase code orchestrating action control that will appear stochastic when referenced to

464   external or overt events such as stimuli or responses.

465   Importantly, we have shown that high synchronicity is prominently and consistently observed in the

466   SMAs but significant differences were also observed in the anterior cingulate cortex and the temporal

467   lobe of individual subjects (fig. 2a). This result suggests that the SMAs do not operate in isolation

468   during action switching, but form part of a broader functional network that involves sensory and

469   mnemonic processes. Indeed it has been suggested that the dorsal part of the ACC could play a major

470   role in conflict resolution by facilitating the selection of task relevant information during high conflict

471   decisions (31,55). The consistency between the activity in the ACC and SMAs we observe (fig. 3-a)

472   supports this hypothesis and the existence of a functional connection between the two areas (55,56).

473   In addition, it has been recently shown that the medial frontal cortex can flexibly recruit the medial

474   temporal lobe during decision-making by means of phase synchrony in the theta band (34). This

475   dynamic functional link between mnemonic and motor processes could explain the higher ITPC in

476   the temporal lobe found in our data (fig. 3-A) and suggests the involvement of this area in supporting

477   the mnemonic aspects related to the task (e.g. to recall what action should be performed when an

478   unexpected cue is presented).

479   More generally, phase coding has been acknowledged in the human hippocampus and temporal lobe

480   in mnemonic processes. In particular, (57) found that oscillations in the theta band reset their cycle

481   after stimulus presentation, leading to strong patterns of inter-trial phase coherence that correlate

482   with memory encoding. Similar phase resets in the theta range are found in frontal circuits with

483   greater synchrony underlying correct trials (58) and are thought to mediate attentional shifts. The

484   temporal patterns found in our study could, therefore, be the result of a switch cue induced phase

485   reset, encoding action related information, where the magnitude of the reset and its entrainment of

16

486   local activity drives faster motor responses. The cycle of theta oscillations could indeed carry
487   patterns of information by modulating the amplitude of higher-frequencies in the gamma range (24).
488   Theta-gamma code is believed to represent a fundamental information-processing mode of the brain
489   responsible for sequential item encoding long-term and working memory within memory areas (59).
490   Recently, signatures of the theta-gamma code have been found in frontal cortical circuits during
491   cognitive control tasks. (12) for example, found increased theta-gamma phase-amplitude coupling
492   between prefrontal and motor regions when decisions followed higher order rules. Few reports have
493   linked phase coding to single trial behavioral performance, as in (15) where the strength of phase-
494   amplitude coupling in frontal and parietal regions correlated with reaction times during the
495   allocation of visuospatial attention. Similarly, we report distinct theta-gamma coupling modulated by
496   behavioral performance which suggests that theta range activity reflects a cognitive control signal
497   that entrains the gamma frequency activity of local neuronal populations (35).

498   Altogether these results contribute to a growing body of literature that identifies frontal theta phase
499   coding as a mechanism promoting cognitive control of behavior (11). Low-frequency oscillations
500   indeed could be a means of information exchange across distant populations within the same
501   functional network (13,35). For example, (16) found fronto-parietal theta synchrony in primate in
502   primate to be predictive of the ability to correctly switch from automatic to deliberate control.
503   However, differently from our analysis, they did not find a relationship with the response time. A
504   similar synchronization pattern was found between the medial frontal cortex and the basal ganglia
505   (60).

506   Low-frequency oscillatory patterns could also be the result of cortical travelling waves in the theta
507   and alpha bands that have been identified as a mechanism through which information propagates
508   throughout cortical networks (61). Importantly, the spatial and temporal consistency of travelling
509   waves in the prefrontal cortex has been shown to have a facilitatory effect on working memory
510   retrieval, with greater synchrony predicting faster responses (21). Our results suggest a similar effect
511   within supplementary-motor circuits with phase synchrony having a facilitatory effect on deliberate
512   behavior. Contrary to this hypothesis, it has been suggested that medial-frontal theta oscillations may
513   also reflect inhibitory control by mediating action-slowing during situations of conflict and error (9).
514   In particular, human EEG studies testing interference tasks reported increased power in the theta
515   range during high-conflict trials correlating with an increase in response time, both prospectively
516   and retrospectively (i.e. post-error slowing) (8–10). Even though we did not explicitly test for this
517   aspect within our paradigm, we cannot confirm the role of theta as a signature of inhibition for three
518   reasons. Firstly, our analysis did not reveal any distinctive role of theta oscillatory power. In addition,
519   theta oscillatory phase alignment was found to reduce rather than increasing the response time on
520   deliberate switch trials. Finally, in our experiment, the detected pattern of synchronized activity
521   emerged by aligning the LFP of each trial to the peak of an action related event. If theta
522   synchronization represented an inhibitory signal, this event would not be strictly dependent on

17

523   action execution and it would be expected to rise consistently earlier than the peak of the MRCP (62).

524   This discrepancy might again be due to the differences in resolution and specificity of iEEG versus

525   EEG recordings.

526   Overall, our results suggest that within frontal cortical networks, theta oscillations encode a control

527   signal that promotes the execution of deliberate actions. In particular, we propose that the power

528   and phase of theta oscillations may reflect different functional roles, where the former locally

529   encodes a general conflict signal and the latter serves as a long-range communication channel

530   facilitating cognitive control (63). This proposal is in agreement with recent accounts of cognitive

531   control that essentially see action selection (i.e. facilitation) and inhibition as two faces of the same

532   coin and therefore postulate complementary neural mechanism underlying these functions (64,65)

533   such as the power and phase of theta band oscillations. This further confirms that phase coding is a

534   fundamental representational format deployed by the brain.

535

536

537   **METHODS**

538

539   **Data collection**

540

541   Data were collected from three right-handed subjects with intractable epilepsy, temporarily

542   implanted with intracranial electrodes (iEEG) as a part of a pre-operation procedure to localize the

543   seizure focus. Electrode placement was determined by the surgeons based on the clinical need of

544   each patient.

545   Data were recorded at the Epilepsy Monitoring Unit of the Hospital del Mar, Barcelona, Spain. All

546   subjects provided the informed consent to participate in the study in accordance with the ethical

547   committee of the Pompeu Fabra University as well as Hospital del Mar. All iEEG recordings were

548   performed using a standard clinical EEG system (XLTEK, subsidiary of Natus Medical) with a 500 Hz

549   sampling rate. A uni- or bilateral implantation was performed using 12 to 16 intracerebral electrodes

550   (Dixi Médical, Besançon, France; diameter: 0.8 mm; 5 to 15 contacts, 2 mm long, 1.5 mm apart) that

551   were stereotactically inserted using robotic guidance (ROSA, Medtech Surgical, Inc).

552

553   To identify the anatomical position of the electrode contacts we used the 3D Slicer software(66).

554   With the registration tool, we coregistered (rigid body, 6 degrees of freedom) the post-implantation

555   CT scan to the pre-implantation MRI. We then added the electrode fiducials on a glass model of each

556   patient's brain obtained with the segmentation tool of the Freesurfer bundle (67). To obtain a single

557   model we coregistered all studies on the MNI152 template provided by the Freesurfer bundle using a

558   semi-automated registration process of 3D Slicer. Briefly, we calculated a linear transform with 12

559   degrees of freedom by superposing and morphing each patient's brain MRI onto the MNI brain

560 template, then we used the transform matrix to translate, shift, skew and resize all other studies (CT

561 scan, and unaltered MRI) accordingly. Since the 3D Slicer interface shows the MNI coordinates when

562 hovering the mouse pointer, we could identify structures touched by electrode contacts both by

563 visual inspection and by referring to the aforementioned coordinates.

564

565

566 **Behavioral task**

567

568 The behavioral task was a variation of the standard Serial Reaction Time Task (SRTT), a type of

569 paradigm that promotes automation of sequential motor behavior (17). Differently from the original

570 task, however, here, in a small subset of trials, the sequential automated action was occasionally

571 interrupted by a cue that required the subjects to switch to a different goal instructed at the

572 beginning of the experiment.

573 The task comprised a maximum of 500 experimental trials preceded by 60 trials of training. There

574 were two types of trials: automatic and switch. Every trial started with a waiting period of 700 ms +-

575 200 ms during which the screen remained blank. After this, subjects were presented with a virtual 4

576 by 4 square keyboard.

577 During automatic trials, a sequence of five keys was highlighted sequentially (green cue) upon

578 button-press. Subjects were instructed to press the cued key as rapidly as possible until the end of

579 the sequence. Each trial terminated at the end of the sequence, and the following one started. The

580 sequence was pseudorandomly generated at the beginning of the experiment to respect a spatial

581 uniform distribution over the keyboard and it was maintained constant throughout the experiment.

582 Switch trials started with the same highlighted key as the automatic trials (green cue), and the next

583 step in the sequence was highlighted upon a button press. Differently from automatic trials, however,

584 one of the intermediate steps of the sequence (i.e. step 2-4 selected at random) highlighted in red

585 (switch cue). Upon presentation of the switch cue, subjects were required to halt the ongoing

586 sequence of movements as fast as possible and press an alternative, uncued key. Participants

587 received all the instructions prior to the beginning of the experiment. Feedback was provided for

588 neither the correct nor incorrect performance. The training phase only comprised automatic trials,

589 whereas the experimental phase included a combination of automatic and switch trials pseudo-

590 randomly interspersed every 7 +-2 trials.

591 The experimental setup ran on a portable capacitive screen fixed to the hospital overbed table. The

592 tablet included a custom-made Java-based application running the experimental task and logged

593 behavioral performance at 50 Hz whereas task synchronization with the neural recordings was

594 achieved through serial communication with the recording system. Subjects sat in a comfortable

595 position that avoided motor constraints to the arm. After receiving the instructions, subjects

596   underwent a short session that exemplified the task. After this, the experimental session started.

597   Subjects could withdraw at any point during the task.

598

599

600   **Electrophysiology pre-processing**

601

602   All electrophysiological data were preprocessed in Matlab (EEGLAB toolbox) and subsequently

603   analyzed in Python using custom scripts based on the Numpy , Scipy , SkLearn and MNE libraries.

604   Data were initially filtered using a two-way zero phase-lag, FIR bandpass filter (2-200 HZ) and an

605   additional notch filter (window = 2Hz) at 50Hz, 100Hz and 150Hz to remove AC current

606   contamination and respective harmonics. Following this step, the signals were individually re-

607   referenced to the average potential of all electrodes for each subject.

608   After filtering, artifacts derived from strong muscle activity or interference due to contact with

609   electrical devices were identified by visual inspection and respective epochs rejected. To reduce

610   remaining artifacts (i.e. cardiac artifacts, muscle twitches), we applied a combination of Principal

611   Component Analysis (PCA) and independent component analysis (ICA). In brief, we performed PCA

612   on all channels and identified those components which accounted for > 98% of the variance. Such

613   components were subsequently decomposed into the same number of independent components

614   through ICA. At this point, each component time series was visually inspected and components that

615   reflected signal artifacts were rejected. The selection of artifact components was based on a careful

616   inspection of their power spectrum, correlation with other physiological measures (i.e. ECG), and the

617   relation to the temporal structure of the experiment. The rejection was performed by setting the ICA

618   weight associated to the artifact component to 0. The signal was further reconstructed by inverting

619   the ICA operation and the subsequent PCA operation after having renormalized the remaining

620   weights.

621

622

623   **Amplitude analysis**

624

625   For each subject, the filtered and artifact-free signal was split into epochs according to the trial

626   structure of the task. Each epoch was individually baseline corrected by subtracting the mean

627   amplitude value in a temporal window of 500 ms preceding the beginning of each trial. To identify

628   task-selective channels displaying changes in the amplitude of the signal (i.e. Movement Related

629   Cortical Potentials (MRCP)) we extracted a set of 3 descriptors (absolute mean, variance and

630   integral) and assigned binary labels to each epoch according to the trial type (0=automatic,

631   1=switch). Further, we applied a classification method based on the Linear Discriminant Analysis

632   (LDA) (68). 100 cross-validation steps were performed to assess performance with Fishers F1 score

633   on class-balanced bootstraps of data samples (80% training, 20% testing). The channels providing

634   the highest classification accuracy were finally selected as the task-related channels. Note that this

635   analysis was naive with regards to the electrode location or the polarity of the event. This step

636   allowed us to narrow down our analysis to those contact points that displayed a task-related change

637   in the amplitude (a detectable difference between conditions) for each subject.

638   Spectral analysis revealed the presence of MRCPs in the low-frequency range between 1 and 2 Hz

639   (not shown). Trial-by-trial MRCP peaks in the switch condition were therefore identified by low-

640   passing the signal up to 2 Hz using a two-ways zero-phase FIR filter and applying a peak detection

641   algorithm that estimated the time of the absolute peak amplitude in the interval between stimulus

642   presentation (switch-cue) and the response. Single-trial stimulus-peak interval, as well as peak-

643   response interval, were further calculated by subtracting the stimulus presentation time from the

644   peak time and the peak time from the response time respectively.

645   Finally, the statistical analysis of amplitude differences was performed through a T-statistics one-

646   dimensional non-parametric cluster based permutation test (30) as implemented in the MNE toolbox

647   with cluster significance threshold = 0.05 and number of permutations = 1000.

648

649

650   **Spectral Analysis**

651

652   Spectral analyses were performed using a DPSS multi-taper method (69,70) as implemented in the

653   MNE toolbox. Trials were aligned to the relative MRCPs peak time, rather than to the behavioral

654   response, in order to avoid artifacts due to the averaging temporally variable signal (19). Changes in

655   the power with respect to the baseline where computed by z-transforming the power spectrum.

656   Statistical differences in the time-frequency power between conditions were calculated through T-

657   statistics two-dimensional cluster based permutation analysis as implemented in the MNE toolbox

658   setting cluster significance threshold = 0.05 and number of permutations = 1000 (30).

659

660

661   **Inter-trial phase coherence (ITPC)**

662

663   We estimated inter-trial phase coherence to quantify the frequency-dependent synchronization

664   across MRCP peak-aligned trials through Phase Locking Value (PLV) method (71). ITCP is computed

665   as:

666

$$ITPC = \frac{1}{N} \left| \sum_{n=1}^{N} e^{j\phi_n} \right|$$

21

667

668   where N is the number of trials in one condition and ϕ represents the phase estimate at the nth trial.

669   ITCP is bounded between 0 and 1, where 1 represents full phase synchronization. In order to test

670   differences in ITCP between conditions, we used the cluster-based permutations method proposed

671   by (30). First, we applied a z-transform to the difference in coherence between conditions (Z_{ITPC}) that

672   rendered the distribution approximately normal (72):

673

$$Z_{ITPC} = \frac{\left(tanh^{-1}(|ITPC_1|) - (1/df_1 - 2)\right) - \left(tanh^{-1}(|ITPC_2|) - (1/df_2 - 2)\right)}{\sqrt{(1/df_1 - 2) + (1/df_2 - 2)}}$$

674

675

676   Where $ITPC_i$ and df_i represent the inter-trial phase coherence and degrees of freedom for the ith

677   condition respectively. To account for the positive bias of ITPC, we used the same amount of trials for

678   the two conditions compared. Second, we selected those regions where z>2.58 corresponding to the

679   99th percentile of the distribution. Finally, we assessed the significance of the measured difference

680   against the H0 obtained by computing the coherence difference between surrogate groups

681   constructed by permuting 1000 times the original labels and extracting the resulting Montecarlo P

682   value.

683

684

685   **Single trial ITPC**

686

687   ITPC is by definition an average measure across multiple trials. An estimate of the contribution of the

688   single trial to the average ITPC (STPC), however, can be obtained by computing the difference

689   between the ITPC across all trials and the ITPC across all but one trial following the method proposed

690   by (23) and previously applied by (22). The Single Trial ITPC ($STPC_i$) for the ith trial is computed as

691   follows:

692

$$STPC_i = N\, Z_{itpc}^{all} - (N - 1)\ Z_{itpc}^{all-i}$$

693

694   where N is the number of trials and Z_{itpc}^{all} and Z_{itpc}^{all-1} are the z-transformed ITPCs for all trials and all

695   but the ith trial respectively. Finally, we computed the STPC for each trial and time-frequency bin.

696   The correlation coefficient between STPC and single trial reaction times was calculated using the

697   Spearman's R, as the STPC distribution was found to violate the normality assumption. This

698   operation was repeated in order to cover the whole time-frequency range, resulting in an R map of

699   size time - frequency.

22

700   To further compute the statistical significance of the obtained R map and to correct for multiple
701   comparisons we applied cluster permutation analysis for each subject. In brief, for each bin we
702   randomly shuffled the data on both the reaction time and the STPC dimensions and recomputed at
703   each permutation the Spearman's R for a total of 1000 permutations. For each bin we obtained a
704   distribution of R under random condition, which served to set the threshold of significance to the
705   99% percentile of the distribution, corresponding to a p value of 0.01. Further, each randomly
706   obtained R map was thresholded according to the corresponding significant value, so to obtain a
707   number of time-frequency clusters where the correlation coefficient was found significant. To
708   determine whether the thresholded time-frequency clusters obtained from the experimental
709   condition could be considered statistically significant we compared their magnitude with the ones
710   resulted from the permutation analysis. To this end, for each cluster we integrated the absolute R
711   value so to obtain one magnitude value per cluster. Further we computed the distribution of cluster
712   magnitudes under random condition and calculated its 99% percentile, corresponding to a p value of
713   0.01. Cluster magnitudes in the experimental condition that exceeded this threshold were considered
714   statistically significant. Whole brain maps were obtained by projecting the average z score of those
715   individual contact points showing a significant cluster in the time window between -0.6 and 0.4 s in
716   the MNI space.

717

718   **Phase-amplitude coupling (PAC)**

719

720   PAC is a measure that quantifies the modulatory effect of low-frequency phase on higher frequency
721   amplitude as a signature of the interaction between their underlying processes resonating at
722   different frequency bands. PAC was computed through the Generalized Linear Models (GLM) method
723   (37) that captures the proportion of variance explained by an underlying linear relationship between
724   analytical amplitude (i.e. envelope, modulated) and phase (modulating) as obtained by Hilbert
725   transforming the signal, using the PACpy toolbox (https://github.com/voytekresearch/pacpy).
726   We restricted our analysis of PAC to the ROIs emerged from cluster-based permutation analysis and
727   selected as modulatory frequency band the significant frequency domain range for each subject. Our
728   epoch selection was also restricted to the temporal window of approximately 400 ms where a
729   significant increase in phase alignment was detected. For each subject, we obtained one surrogate
730   signal for fast and slow trials by concatenating the respective single trial windows, so to achieve the
731   temporal resolution necessary for this type of analysis. Further, we computed PAC values between
732   the selected modulatory phase and the amplitude of higher frequencies (10-100 Hz in steps of 2 Hz,
733   modulated frequency), and obtained the difference between the two conditions.
734   Statistical significance between the two conditions was tested through z-statistics against the null-
735   hypothesis of samples from both conditions belonging to the same distribution. This was obtained by
736   randomly permuting the conditions' labels and calculating the 95 percentile of the maximum PAC

737   value achieved under the assumption that the two conditions were sampled from the same

738   distribution (38). Note that this approach could introduce spurious oscillations as an artifact due to

739   the concatenation of several signals, where the frequency of the oscillation is directly proportional to

740   the length of the segments concatenated. We control for this possibility by choosing temporal

741   windows that may introduce artifacts at lower frequencies than those considered in this analysis. In

742   addition, the same concatenation is applied equally for both conditions and therefore it is unlikely to

743   affect the comparison.

744

745

746   **ACKNOWLEDGMENTS**

747

753

754

755

756   **COMPETING INTERESTS**

757

758   The authors declare no competing interests

759

760   **REFERENCES**

761

762   1.   Rushworth MFS, Hadland KA. Role of the Human Medial Frontal Cortex in Task Switching: A

763   Combined fMRI and TMS Study. J …. 2002;2577–92.

764   2.   Rushworth MFS, Walton ME, Kennerley SW, Bannerman DM. Action sets and decisions in the

765   medial frontal cortex. Trends Cogn Sci. Thieme; 2004 Sep;8(9):410–7.

766   3.   Nachev P, Kennard C, Husain M. Functional role of the supplementary and pre-supplementary

767   motor areas. Nat Rev Neurosci. 2008;9(11):856–69.

768   4.   Hikosaka O, Isoda M. Switching from automatic to controlled behavior: cortico-basal ganglia

769   mechanisms. Trends Cogn Sci. Elsevier Ltd; 2010;14(4):154–61.

770   5.   Sakai K. Task Set and Prefrontal Cortex. Annu Rev Neurosci. Annual Reviews ; 2008 Jul

771   17;31(1):219–45.

772   6.   Isoda M, Hikosaka O. Switching from automatic to controlled action by monkey medial frontal

773   cortex. Nat Neurosci. Nature Publishing Group; 2007 Feb;10(2):240–8.

774   7.   Roberts RE, Husain M. A dissociation between stopping and switching actions following a
775   lesion of the pre-supplementary motor area. Cortex. Elsevier Ltd; 2015;63:184–95.
776   8.   Cohen MX, Cavanagh JF. Single-trial regression elucidates the role of prefrontal theta
777   oscillations in response conflict. Front Psychol. 2011;2(FEB):1–12.
778   9.   Cavanagh JF, Frank MJ. Frontal theta as a mechanism for cognitive control. Trends Cogn Sci.
779   Elsevier Ltd; 2014;18(8):414–21.
780   10.   Narayanan NS, Cavanagh JF, Frank MJ, Laubach M. Common medial frontal mechanisms of
781   adaptive control in humans and rodents. Nat Neurosci. Nature Publishing Group;
782   2013;16(12):1888–95.
783   11.   Helfrich RF, Knight RT. Oscillatory Dynamics of Prefrontal Cognitive Control. Trends Cogn Sci.
784   Elsevier Ltd; 2016;20(12):916–30.
785   12.   Voytek B, Kayser AS, Badre D, Fegen D, Chang EF, Crone NE, et al. Oscillatory dynamics
786   coordinating human frontal networks in support of goal maintenance. Nat Neurosci. Nature
787   Publishing Group; 2015;18(9):1318–24.
788   13.   Smith EH, Horga G, Yates MJ, Mikell CB, Banks GP, Pathak YJ, et al. Widespread temporal
789   coding of cognitive control in the human prefrontal cortex. Nat Neurosci. Nature Publishing
790   Group; 2019 Nov 30;22(11):1883–91.
791   14.   Sweeney-Reed CM, Zaehle T, Voges J, Schmitt FC, Buentjen L, Kopitzki K, et al. Thalamic theta
792   phase alignment predicts human memory formation and anterior thalamic cross-frequency
793   coupling. Elife. eLife Sciences Publications Limited; 2015 May 20;4:e07578.
794   15.   Szczepanski SM, Crone NE, Kuperman RA, Auguste KI, Parvizi J, Knight RT. Dynamic Changes
795   in Phase-Amplitude Coupling Facilitate Spatial Attention Control in Fronto-Parietal Cortex.
796   PLoS Biol. 2014;12(8).
797   16.   Phillips JM, Vinck M, Everling S, Womelsdorf T. A long-range fronto-parietal 5- to 10-Hz
798   network predicts "top-down" controlled guidance in a task-switch paradigm. Cereb Cortex.
799   2014;24(8):1996–2008.
800   17.   Nissen MJ, Bullemer P. Attentional requirements of learning: Evidence from performance
801   measures. Cogn Psychol. 1987 Jan;19(1):1–32.
802   18.   Hallett M. Movement-related cortical potentials. Electromyogr Clin Neurophysiol.
803   1994;34(1):5–13.
804   19.   van Diepen RM, Mazaheri A. The Caveats of observing Inter-Trial Phase-Coherence in
805   Cognitive Neuroscience. Sci Rep. Nature Publishing Group; 2018 Dec 14;8(1):2990.
806   20.   Alexander DM, Jurica P, Trengove C, Nikolaev AR, Gepshtein S, Zvyagintsev M, et al. Traveling
807   waves and trial averaging: The nature of single-trial and averaged brain responses in large-
808   scale cortical signals. Neuroimage. 2013 Jun;73:95–112.
809   21.   Zhang H, Watrous AJ, Patel A, Jacobs J, Zhang H, Watrous AJ, et al. Theta and Alpha Oscillations
810   Are Traveling Waves in the Human Neocortex Article Theta and Alpha Oscillations Are

811   Traveling Waves in the Human Neocortex. Neuron. Elsevier; 2018;98(6):1269–1281.e4.

812   22.   Hipp JF, Engel AK, Siegel M. Oscillatory Synchronization in Large-Scale Cortical Networks

813   Predicts Perception. Neuron. 2011 Jan 27;69(2):387–96.

814   23.   Jarvis MR, Mitra PP. Sampling properties of the spectrum and coherency of sequences of

815   action potentials. Neural Comput. 2001 Apr;13(4):717–49.

816   24.   Lisman JE, Jensen O. The θ-γ neural code. Neuron. NIH Public Access; 2013 Mar

817   20;77(6):1002–16.

818   25.   Lee D. Behavioral context and coherent oscillations in the supplementary motor area. J

819   Neurosci. Society for Neuroscience; 2004 May 5;24(18):4453–9.

820   26.   Sakai K, Hikosaka O, Nakamura K. Emergence of rhythm during motor learning. Trends Cogn

821   Sci. 2004;8(12):547–53.

822   27.   Tanji J. Sequential Organization of Multiple Movements: Involvement of Cortical Motor Areas.

823   Annu Rev Neurosci. 2001;24(1):631–51.

824   28.   Karimi F, Kofman J, Mrachacz-Kersting N, Farina D, Jiang N. Detection of Movement Related

825   Cortical Potentials from EEG Using Constrained ICA for Brain-Computer Interface

826   Applications. Front Neurosci. Frontiers Media SA; 2017;11:356.

827   29.   Lopour BA, Tavassoli A, Fried I, Ringach DL. Coding of Information in the Phase of Local Field

828   Potentials within Human Medial Temporal Lobe. Neuron. Cell Press; 2013 Aug 7;79(3):594–

829   606.

830   30.   Maris E, Schoffelen J-M, Fries P. Nonparametric statistical testing of coherence differences. J

831   Neurosci Methods. 2007 Jun;163(1):161–75.

832   31.   Mansouri FA, Tanaka K, Buckley MJ. Conflict-induced behavioural adjustment: A clue to the

833   executive functions of the prefrontal cortex. Nature Reviews Neuroscience. Nature Publishing

834   Group; 2009. p. 141–52.

835   32.   Murty VP, LaBar KS, Adcock RA. Distinct medial temporal networks encode surprise during

836   motivation by reward versus punishment. Neurobiol Learn Mem. Academic Press Inc.; 2016

837   Oct 1;134(Part A):55–64.

838   33.   Berkers RMWJ, Klumpers F, Fernández G. Medial prefrontal–hippocampal connectivity during

839   emotional memory encoding predicts individual differences in the loss of associative memory

840   specificity. Neurobiol Learn Mem. Academic Press Inc.; 2016 Oct 1;134:44–54.

841   34.   Minxha J, Adolphs R, Fusi S, Mamelak AN, Rutishauser U. Flexible recruitment of memory-

842   based choice representations by the human medial frontal cortex. Science (80-). American

843   Association for the Advancement of Science; 2020 Jun 26;368(6498).

844   35.   Canolty RT, Knight RT. The functional role of cross-frequency coupling. Trends Cogn Sci. 2010

845   Nov;14(11):506–15.

846   36.   Hyafil A, Giraud AL, Fontolan L, Gutkin B. Neural Cross-Frequency Coupling: Connecting

847   Architectures, Mechanisms, and Functions. Trends Neurosci. Elsevier Ltd; 2015;38(11):725–

848   40.

849   37.   Penny WD, Duzel E, Miller KJ, Ojemann JG. Testing for nested oscillation. J Neurosci Methods.
850   2008 Sep 15;174(1):50–61.

851   38.   Maris E, Oostenveld R. Nonparametric statistical testing of EEG- and MEG-data. J Neurosci
852   Methods. 2007 Aug 15;164(1):177–90.

853   39.   Moisello C, Crupi D, Tunik E, Quartarone A, Bove M, Tononi G, et al. The serial reaction time
854   task revisited: A study on motor sequence learning with an arm-reaching task. Exp Brain Res.
855   2009;194(1):143–55.

856   40.   Keele SW, Ivry R, Mayr U, Hazeltine E, Heuer H. The cognitive and neural architecture of
857   sequence representation. Psychol Rev. 2003;110(2):316–39.

858   41.   Crone EA, Wendelken C, Donohue SE, Bunge SA. Neural evidence for dissociable components
859   of task-switching. Cereb Cortex. 2006;16(4):475–86.

860   42.   Monsell S. Task switching. Trends Cogn Sci. 2003;7(3):134–40.

861   43.   Buzsáki G, Anastassiou CA, Koch C. The origin of extracellular fields and currents — EEG ,
862   ECoG , LFP and spikes. Nature Publishing Group; 2012;13(June):407–20.

863   44.   Sumner P, Nachev P, Morris P, Peters AM, Jackson SR, Kennard C, et al. Human Medial Frontal
864   Cortex Mediates Unconscious Inhibition of Voluntary Action. Neuron. Elsevier Inc.;
865   2007;54(5):697–711.

866   45.   RUSHWORTH M, WALTON M, KENNERLEY S, BANNERMAN D. Action sets and decisions in
867   the medial frontal cortex. Trends Cogn Sci. 2004 Sep;8(9):410–7.

868   46.   Rushworth MFS, Hadland KA, Paus T, Sipila PK. Role of the Human Medial Frontal Cortex in
869   Task Switching: A Combined fMRI and TMS Study. J Neurophysiol. 2002 May;87(5):2577–92.

870   47.   Kornhuber HH, Deecke L. Hirnpotentialänderungen bei Willkürbewegungen und passiven
871   Bewegungen des Menschen: Bereitschaftspotential und reafferente Potentiale. Pflugers Arch
872   Gesamte Physiol Menschen Tiere. 1965;284(1):1–17.

873   48.   Shibasaki H, Hallett M. What is the Bereitschaftspotential? Clinical Neurophysiology. Clin
874   Neurophysiol; 2006. p. 2341–56.

875   49.   Colebatch SKJJG. Movement-related potentials associated with self-paced , cued and imagined
876   arm movements. 2002;98–107.

877   50.   Schurger A, Mylopoulos M, Rosenthal D. Neural Antecedents of Spontaneous Voluntary
878   Movement: A New Perspective. Trends Cogn Sci. Elsevier; 2016 Feb 1;20(2):77–9.

879   51.   LIBET B, GLEASON CA, WRIGHT EW, PEARL DK. TIME OF CONSCIOUS INTENTION TO ACT IN
880   RELATION TO ONSET OF CEREBRAL ACTIVITY (READINESS-POTENTIAL). Brain. 1983
881   Sep;106(3):623–42.

882   52.   Schurger A, Sitt JD, Dehaene S. An accumulator model for spontaneous neural activity prior to
883   self-initiated movement. Proc Natl Acad Sci U S A. National Academy of Sciences; 2012 Oct
884   16;109(42):E2904-13.

885   53.   Delorme A, Westerfield M, Makeig S. Medial Prefrontal Theta Bursts Precede Rapid Motor
886   Responses during Visual Selective Attention. J Neurosci. 2007;27(44):11949–59.

887   54.   Ramchurn A, de Fockert JW, Mason L, Darling S, Bunce D. Intraindividual reaction time
888   variability affects P300 amplitude rather than latency. Front Hum Neurosci. Frontiers; 2014
889   Jul 29;8:557.

890   55.   Swick D, Turken U. Dissociation between conflict detection and error monitoring in the
891   human anterior cingulate cortex. Proc Natl Acad Sci U S A. National Academy of Sciences;
892   2002 Dec 10;99(25):16354–9.

893   56.   Picard N, Strick PL. Motor areas of the medial wall: A review of their location and functional
894   activation. Cerebral Cortex. Cereb Cortex; 1996. p. 342–53.

895   57.   Rizzuto DS, Madsen JR, Bromfield EB, Schulze-Bonhage A, Seelig D, Aschenbrenner-Scheibe R,
896   et al. Reset of human neocortical oscillations during a working memory task. Proc Natl Acad
897   Sci U S A. National Academy of Sciences; 2003 Jun 24;100(13):7931–6.

898   58.   Voloh B, Valiante TA, Everling S, Womelsdorf T. Theta-gamma coordination between anterior
899   cingulate and prefrontal cortex indexes correct attention shifts. Proc Natl Acad Sci U S A.
900   National Academy of Sciences; 2015 Jul 7;112(27):8457–62.

901   59.   Fell J, Axmacher N. The role of phase synchronization in memory processes. Nat Rev Neurosci.
902   2011 Feb 20;12(2):105–18.

903   60.   Zavala B, Tan H, Ashkan K, Foltynie T, Limousin P, Zrinzo L, et al. Human subthalamic nucleus-
904   medial frontal cortex theta phase coherence is involved in conflict and error related cortical
905   monitoring. Neuroimage. The Authors; 2016;137:178–87.

906   61.   Muller L, Chavane F, Reynolds J, Sejnowski TJ. Cortical travelling waves: mechanisms and
907   computational principles. Nat Rev Neurosci. Nature Publishing Group; 2018 May
908   22;19(5):255–68.

909   62.   Isoda M, Hikosaka O. Role for subthalamic nucleus neurons in switching from automatic to
910   controlled eye movement. J Neurosci. Society for Neuroscience; 2008 Jul 9;28(28):7209–18.

911   63.   Cohen MX. A neural microcircuit for cognitive conflict detection and signaling. Trends
912   Neurosci. Elsevier Ltd; 2014;37(9):480–90.

913   64.   Jasinska AJ. Automatic inhibition and habitual control : alternative views in neuroscience
914   research on response inhibition and inhibitory control INHIBITION CAN BE EITHER A
915   CONTROL PROCESS (TO OVERRIDE A PREPOTENT RESPONSE TENDENCY) PROCESSES
916   MEDIATING RESPONSE INHI. 2013;7(April):1–4.

917   65.   Kenner NM, Mumford JA, Hommer RE, Skup M, Leibenluft E, Poldrack RA. Inhibitory motor
918   control in response stopping and response switching. J Neurosci. Society for Neuroscience;
919   2010 Jun 23;30(25):8512–8.

920   66.   Fedorov A, Beichel R, Kalpathy-Cramer J, Finet J, Fillion-Robin J-C, Pujol S, et al. 3D Slicer as an
921   image computing platform for the Quantitative Imaging Network. Magn Reson Imaging. 2012

922   Nov;30(9):1323–41.

923   67.   Fischl B. FreeSurfer. Neuroimage. 2012 Aug 15;62(2):774–81.

924   68.   Blankertz B, Lemm S, Treder M, Haufe S, Müller K-R. Single-trial analysis and classification of

925   ERP components — A tutorial. Neuroimage. 2011 May 15;56(2):814–25.

926   69.   Mitra PP, Pesaran B. Analysis of Dynamic Brain Imaging Data. Biophys J. 1999 Feb;76(2):691–

927   708.

928   70.   Thomson DJ. Spectrum estimation and harmonic analysis. Proc IEEE. 1982;70(9):1055–96.

929   71.   Lachaux J-P, Rodriguez E, Martinerie J, Varela FJ. Measuring phase synchrony in brain signals.

930   Hum Brain Mapp. John Wiley & Sons, Ltd; 1999 Jan 1;8(4):194–208.

931   72.   Enochson LD, Goodman NR. CeqQ GAUSSIAN APPROXIMATIONS TO THE DISTRIBUTION OF

932   SAMPLE COHERENCE. 1965 Jun.

933